Molecular modeling of intermolecular and intramolecular excluded volume interactions for polymers at interfaces

M. Charlaganov and F. A. M. Leermakers[a)]
Laboratory of Physical Chemistry and Colloid Science, Wageningen University, Dreijenplein 6, Wageningen 6703HB, The Netherlands

(Received 13 October 2009; accepted 1 December 2009; published online 30 December 2009)

A hybrid modeling approach is proposed for inhomogeneous polymer solutions. The method is illustrated for the depletion problem with polymer chains up to $N=10^3$ segments in semidilute solutions and good solvent conditions. In a three-dimensional volume, a set of freely jointed chains is considered for which the translational degrees of freedom are sampled using a coarse grained Monte Carlo simulation and the conformational degrees of freedom of the chains are computed using a modified self-consistent field theory. As a result, both intramolecular and intermolecular excluded volume effects are accounted for, not only for chains near the surface, but in the bulk as well. Results are consistent with computer simulations and scaling considerations. More specifically, the depletion thickness, which is a measure for the bulk correlation length, scales as $\delta \propto \varphi^{-0.75}$ and converges to the mean field result in the concentrated regime. © *2009 American Institute of Physics*. [doi:10.1063/1.3276286]

I. INTRODUCTION

Covering appropriate length scales in an efficient computational method, without loosing the essential physics, is one of the prominent challenges of polymer physics. There are simulation methods that deal with all degrees of freedom rigorously. It is fair to say, however, that for systems composed of a large number of long polymers these methods are computationally challenging. A reasonable approach then is to solve coarse grained models, wherein a chain is represented by, e.g., a single soft particle.[1] At the down side, however, one will loose information on the length scale smaller than the particle (coil) size. In this paper we propose a fine-graining strategy to recover the information lost in the coarse graining. The idea is to use a MC simulation that operates on just a few (translational) degrees of freedom of the chains and apply the SCF model for the remaining (conformational) ones. Unlike the standard SCF method,[2] the MC-SCF hybrid scheme accounts (in the first order) for both intermolecular as well as intramolecular excluded volume effects. As a test case we consider the polymer depletion problem for which both simulation results and scaling type theory are available.[1,3,4]

II. HYBRID MC-SCF METHOD

There exists a strong analogy between a diffusing particle and an ideal chain. Of course the ideal chain is only a first-order model for the real chain because interactions are fully ignored. SCF methods advance this idea by considering the polymer as an ideal chain in an external field. This field is used to account for interactions of a polymer segment with its average surroundings.[5] For polymers at interfaces this approach is known to give good qualitative results.[2] In good solvent conditions, however, the method fails to account for the swelling of the chains and hence the mean field results fall short to give the correct scaling behavior.[3]

Calculating macroscopic properties of a system always involves averaging. There is a conceptual difference in averaging between conventional simulation techniques such as MC and molecular dynamics methods and the SCF approach. Simulations rigorously consider microstates and calculate the interaction energies in a particular microscopical configuration. Macroscopic quantities are then obtained by averaging over relevant microscopical configurations. In SCF models the external field, that influences the statistical weights of chain conformations, already is based on averaged characteristics. As such the potentials make no difference between interchain and intrachain excluded volume contributions the chains do not swell in good solvents.

There are many different SCF approaches.[6–9] All of these have several aspects in common. Typically, there exists (a) a rule that specifies how to obtain the potential field from the density distribution of components, (b) a rule to find the density distributions of all components for given potential fields, and (c) an algorithm that results in density and a potential distributions that are self-consistent with respect to rules (a) and (b). In particular, the potentials $u(\mathbf{r})$ are self-consistent when the densities derived by using rule (b) yields the same potentials $u(\mathbf{r})$ after applying rule (a). Below we will discuss these three aspects for a new SCF-like theory for which an additional step is introduced that allows us to better account for intermolecular and intramolecular excluded volume effects.

This new approach modifies the standard Scheutjens–Fleer theory[10] on just a few points. We therefore start by presenting the basic steps of the classical theory first. Below we will use dimensionless units. This means that all energies and potentials are normalized by k_BT and all distances are

[a)]Electronic mail: frans.leermakers@wur.nl.

measured in the units of a, where a is the statistical segment length of the polymer. The same value a is chosen as the cell size of a simple cubic lattice. The lattice sites are referred to by their coordinates $\mathbf{r}=x,y,z$ in a Cartesian coordinate system. In a lattice model the natural measure of the segment density or segment concentration is the volume fraction $\varphi(\mathbf{r})$, which may be interpreted as the probability to find a segment at the specified coordinate.

We consider a two component system consisting of a homopolymer and a monomeric good solvent near a nonadsorbing solid wall. As there are no interactions in the system (all Flory–Huggins interaction parameters are zero, $\chi=0$) the solvent and the polymer monomers experience the same (external) potential $u(\mathbf{r})$. The solvent consists of just one segment and its concentration profile $\varphi_W(\mathbf{r})$ follows from the Boltzmann distribution $\varphi_W(\mathbf{r})=C_W G(\mathbf{r})=C_W e^{-u(\mathbf{r})}$, where C_W is a normalization constant. The single segment distribution function $G(\mathbf{r})=e^{-u(\mathbf{r})}$ is introduced here for brevity. Using this result, we find that the potential field can be expressed as a function of the volume fraction of polymer segments $\varphi(\mathbf{r})$

$$u(\mathbf{r}) = \ln C_W - \ln(1-\varphi(\mathbf{r})), \tag{1}$$

where we have used the incompressibility condition $\varphi_W(\mathbf{r})+\varphi(\mathbf{r})=1$.

One can exploit the analogy between random walks and polymer chains to obtain the concentration profile as a function of $u(\mathbf{r})$. Segment ranking numbers $s=1,\cdots,N$ act as step numbers in a three-dimensional random walk problem. The probability to find segment s that belongs to a chain of N segments at coordinate $\mathbf{r}$, is related to the probability that two random walks with lengths s and $N-s+1$, respectively, meet at this position. Using the end point distribution function $G(\mathbf{r},s)$, that represents the statistical weight of all random walks that reach coordinate $\mathbf{r}$ after $s-1$ steps, one can express the polymer volume fraction as

$$\varphi(\mathbf{r}) = \frac{C}{G(\mathbf{r})}\sum_{s=1}^{N} G(\mathbf{r},s)G(\mathbf{r},N-s+1). \tag{2}$$

Here, the normalization constant C ensures that the system contains exactly n chains

$$C = \frac{n}{\Sigma_{\mathbf{r}} G(\mathbf{r},N)}. \tag{3}$$

The single segment distribution function $G(\mathbf{r})$ used in Eq. (2) corrects for double counting of the statistical weight of segment s which contributes to both end point distributions. The end point distribution functions are generated recursively starting from the single segment distribution function, $G(\mathbf{r},1)=G(\mathbf{r})$, and propagates as

$$G(\mathbf{r},s) = \frac{G(\mathbf{r})}{6}\sum_{\mathbf{r}'} G(\mathbf{r}',s-1), \tag{4}$$

where the summation runs over the six coordinates $\mathbf{r}'$ that are nearest neighbors of lattice site $\mathbf{r}$.

Rule (a) to derive u from the concentration profile φ is specified by Eq. (1). Equations (2)–(4) define φ as a functional of u and thus implement rule (b). The iterative procedure that brings these two results to consistency involves making an initial guess for u, then calculating φ, calculating a new guess based on φ and so on until a stationary solution is found. We implemented a Hessian-free Newton-like minimization routine for this task which reaches seven significant digits in order 10^2 iterations.

The boundary conditions are periodic in x and y directions. In the z direction the volume is bounded by two impermeable inert surfaces. For the classical SCF scheme described above these boundary conditions result in a SCF that is uniform in x-y plane. Naturally, this yields a uniform along x and y polymer distribution and a loss of intrachain correlations and a rather primitive account for interchain correlations. This is particularly bad in good solvent conditions and in low polymer concentrations. In semidilute solutions the results remain approximate. Only in the polymer melt, and at theta conditions, the approach is expected to be accurate.

Earlier studies on single chains of different lengths have shown that the intrachain correlations are recovered in SCF calculations with suppressed translational mobility of macromolecules.[11] In these calculations the central segment of the chain was restricted to a single site of the lattice. It was found that the radial volume fraction profile $\varphi(r)$ has various universal features that were long time ago envisioned by de Gennes.[3] There is a central region $0<r<R_g$ where to a good approximation $\varphi(r)=r^{-4/3}$. The volume fraction drops below the overlap value for $r>R_g$ and the profile becomes exponential (with a decay length given by the unperturbed coil size). From the N dependence of the profiles we find, in line with Flory's arguments, that the gyration radius of the two-armed stars obeys the scaling $R_g \propto N^{\alpha}$, with $\alpha \sim 0.6$ and the overlap concentration is found to be consistent with $\varphi^{\mathrm{ov}} \propto N^{-0.8}$.

We extend this approach to the problem of n macromolecules. The chains consist of an odd number of segments N. For each chain i $(i=1,\cdots,n)$ we define a unique lattice site $\mathbf{r}_i$ to which we fix the central segment of the chain.[12]

The restriction to the central segments of the chains is introduced by a modification of the propagation procedure. The restriction sites and constrained segments need special attention while computing the end point distribution functions Eq. (4). More specifically

$$G(\mathbf{r}) = \begin{cases} \sum_{r_i} \delta^{r}_{r_i} & s = \frac{1}{2}(N+1), \\ \left(1-\sum_{r_i}\delta^{r}_{r_i}\right)\exp(-u(r)) & s \neq \frac{1}{2}(N+1), \end{cases} \tag{5}$$

are used instead of the free segment distribution function $G(\mathbf{r})$. With these modifications only chains with central segments in one of the grafting points have nonzero statistical weight and contribute to the polymer density distribution Eq. (2). In passing we note that with these positional constraints, the normalization constant for the solvent in Eq. (1) becomes unity, that is, $C_W=1$.

The free energy F for the n molecules with constrained positions $\{\mathbf{r}_i\}$ is

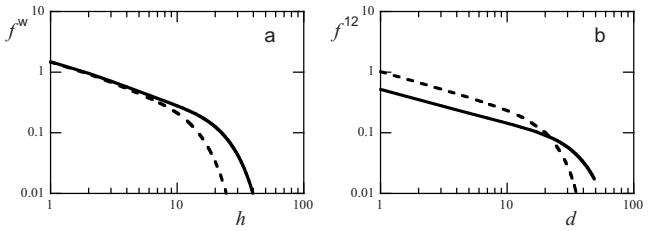

FIG. 1. (a) The gradient of the interaction potential $f^w = \partial F^w / \partial h$ with the surface as a function of the distance h of the central segment to the surface. (b) The gradient of the pair interaction $f^{12} = \partial F^{12}(d) / \partial d$ as a function of the distance d between the two central segments. $N=1001$—solid lines, $N=401$—dashed lines.

$$F(\{\mathbf{r}_i\}) = n \ln C + \sum_{\mathbf{r} \notin \{\mathbf{r}_i\}} \ln \varphi_W(\mathbf{r}), \tag{6}$$

where the coordinates $\mathbf{r}_i$ where the central segments are places are omitted in the sum. Physically, F thus collects the logarithm of the number of conformations lost for the n chains compared to the Gaussian chains. The conformational loss not only comes from the positional constraints on their central segments but also from the interactions between chains which occurs when a chain is near a surface or when two or more neighboring chains partial overlap (interact). Note that the translational entropy of the monomeric solvent is included in Eq. (6) but the corresponding entropy of the polymer chains is not. The next task is thus to introduce translational degrees of freedom for the polymer chains into the problem. Here we suggest to use a MC simulation for this but note that there are various possible alternatives.

At the MC stage, polymer chains are modeled as soft particles interacting with each other and the wall in an effective solvent. The potentials for the simulations are measured in complimentary SCF calculations as is explained next.

Let us consider the problem of bringing (in SCF mode) one isolated chain toward a solid boundary and compute corresponding change in the free energy $F^w(h)$ where h is the distance between the constrained segment of the probe chain and the surface. The wall restricts the conformations of the chain and this gives rise to an entropic repulsion. In Fig. 1(a) we present the derivative $f^w = -\partial F^w / \partial h$ on log-log coordinates which gives the depletion force acting on a single polymer chain. In passing we mention that averaging the polymer concentration profiles for each value of h, $\varphi_h(\mathbf{r})$, collected in this measurement, can be used to obtain the polymer concentration profile in the dilute regime

$$\varphi(z) = C_d \sum_h \sum_{x,y} \varphi_h(x,y,z) e^{-F^w(h)}, \tag{7}$$

where the constant C_d is used to match the desired (low) bulk concentration.

Another essential ingredient that is needed in the MC simulations is the free energy of bringing two chains toward each other. Again, we perform the calculations in a three-dimensional system far away from the boundaries. The central segments of two probe chains are fixed at positions $\mathbf{r}_1$ and $\mathbf{r}_2$, respectively. In SCF mode we obtain the energy of interaction $F^{12}(d)$ where $d = |\mathbf{r}_1 - \mathbf{r}_2|$ is the distance between the two grafting points. The corresponding force, f^{12} is presented in 1b.

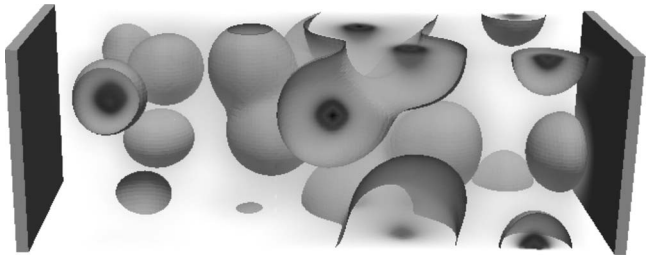

FIG. 2. Volume fraction profile produced in a SCF calculation. $N=1001$, $n=12$, $\varphi^b = 0.033$, the equidensity surface is plotted at $\varphi = 0.034$. The dimensions of the lattice are $51 \times 51 \times 150$ units. Surfaces indicate positions of hard wall boundaries.

The forces $f^{12}(d)$ and $f^w(h)$ presented in Fig. 1 and hence the corresponding potentials have very similar features. For small values of their arguments the forces are inversely proportional to the separation. Therefore a logarithmic dependence is found for the corresponding potentials. This is consistent with simulations and renormalization group theory.[13] At longer distances an exponential decay is found for both F and f, as expected.

The volume in the MC simulations is identical to that in the SCF calculations. There are two surfaces bracketing the z coordinate and periodic boundary conditions in the x and y directions. Here the focus is on n particles that interact with a surface by the $F^w(h)$ potential and suffer a pair potential with the characteristics $F^{12}(d)$. Typically, there are just order 10^2 particles in the volume and thus the simulations are straightforward. Using the standard Metropolis algorithm, an initial equilibration is followed by a production run wherein for a finite number, $j=1,\cdots,J$, with typically $J \approx 10^2$ so-called snapshots, the coordinates $\{\mathbf{r}_i\}_j$ as well as the corresponding prediction of the interaction free energy F_j^{MC} are recorded.[14]

For each snapshot j the SCF equations are solved with the method explained above. Numerically exact volume fraction profiles $\varphi_j(\mathbf{r})$ as well as the free energy F_j^{SCF} were obtained.

An example of a three-gradient volume fraction profile calculated by the (constrained) SCF method is shown in Fig. 2. In this example the centers (which are fixed at specified coordinates that followed from the MC snapshot) of the chains are colored dark and the equivolume fraction contour is plotted for $\varphi = 0.034$ a value close to the bulk volume fraction $\varphi = 0.033$. Clearly the snapshot shows that the chains are not exactly homogeneously distributed in the volume. At some places in the system the chains are near to each other and when the chains overlap the region with volume fraction larger than 0.034 is more extended than in places where the chains are isolated. This indicates that the interchain excluded volume effects are explicitly accounted for. Also clear from this figure is the fact that near the center of each chain the polymer density is higher than the bulk volume fraction and as a result all chains swell as compared to the Gaussian coil size (intramolecular excluded volume effects). In the present example the chains are noninteracting with the two

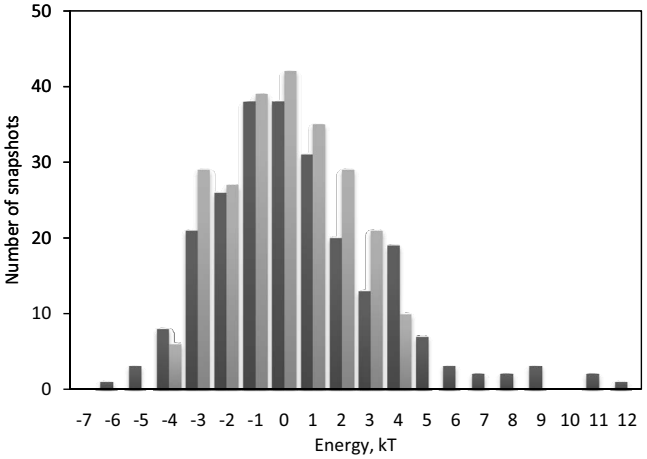

FIG. 3. Distributions of energies of 239 snapshots around median values as estimated on the MC stage (light bars) and calculated on the SCF stage (dark bars). $N=1001$, $n=26$, $\varphi^b=0.069$.

walls. On average the chains avoid the surfaces, as will be discussed below, but this effect cannot easily be seen from a single snapshot. Close inspection of the profiles does reveal the effect of the periodic boundary conditions, chains that are near the boundary "donate" segments to the "opposite" side. In the MC stage only the pair interactions between chains and the interaction between chains and the surface is accounted for. In the (constrained) SCF result, all chains are present and therefore multiple interactions (triplet and higher) are naturally accounted for. This is one of the reasons why in SCF the free energy differs from the "predicted" value of MC.

In Fig. 3 the distributions of free energies for $J=239$ snapshots are shown for both the MC and SCF modes. Both distributions indicate that the snapshots are spread around the median values. The free energy differences $\Delta F_j=F_j^{\mathrm{MC}}-F_j^{\mathrm{SCF}}$ are of order unity, which means that the estimates of the MC train are predictive for the free energy in the SCF calculation.

When the $\{F^{\mathrm{MC}}\}$ would have coincided with those of SCF, we could have performed a flat averaging of the J density profiles $\varphi_j(\mathbf{r})$ to obtain $\varphi(\mathbf{r})$. The subsequent averaging over the x-y plane then results straightforwardly in the normal density profile $\varphi(z)$. However, the energy differences ΔF are not zero and hence we have to correct for the bias

$$\varphi(\mathbf{r})=\frac{\Sigma_j\varphi_j(\mathbf{r})e^{-\Delta F_j}}{\Sigma_j e^{-\Delta F_j}}. \tag{8}$$

III. RESULTS AND DISCUSSION

The primary results from the MC-SCF calculations is the polymer volume fraction (averaged over the x-y plane) profile normal to the surface. Figure 4 presents, for various bulk volume fractions, such profiles for chains with length (a) $N=401$ and (b) $N=1001$. For ease of comparison we have normalized the profiles to the polymer volume fraction in the bulk. Completely in line with expectations we find that the profiles become wider with decreasing polymer concentrations. Also, for dilute polymer concentrations the profiles become wider with increasing chain length. Qualitatively, these trends are well known and completely understood.[2]

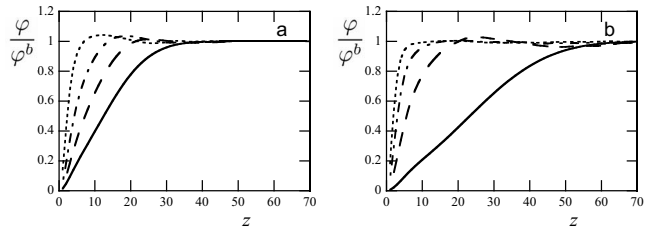

FIG. 4. Polymer concentration profiles normalized by bulk polymer volume fraction. (a) Chain length $N=401$, bulk concentrations 0.05 (dotted line), 0.022 (dot-dash), 0.011 (dashed line), and dilute solution (solid line). (b) Chain length $N=1001$, bulk concentrations 0.069 (dotted line), 0.033 (dot dash), 0.013 (dashed line), and dilute solution (solid line). The relative error of the data points is estimated (Ref. 15) to be $\approx 0.3\%$.

It is of interest to compare the new results to the classical SCF ones. Here we focus on the semidilute regime. It is known that the classical results compare extremely well to analytical predictions that are obtained by using the ground state approximation (GSA).[16] More specifically, to a very good approximation GSA gives $\varphi(z)=\varphi^b\tanh^2(z/\xi)$. Here $\xi=1/\sqrt{3\varphi^b}$ is the mean field correlation length in a semidilute solution, which is a very good measure for the depletion layer thickness. As can be seen in Fig. 5 the differences between the classical SCF and the MC-SCF results are significant. First of all this is because the correlation length and thus the depletion thickness in the MC-SCF method differs noticeably from that in the classical SCF theory [cf. Fig. 5(a)]. Moreover, the MC-SCF result does not fit to the squared hyperbolic tangent profile. In part this is because of a significant oscillatory dependence of the profile, which is discussed below in more detail. Intramolecular excluded volume effects accounted for by MC-SCF and essentially ignored by the classical SCF theory must be the reason for the mentioned differences.

The depletion thickness is an important quantity that can be used to quantify the range over which the polymers feel the surface. A measure of the depletion layer thickness is obtained by taking the first moment over the excess profile

$$\delta=\frac{\Sigma_z z(\varphi(z)-\varphi^b)}{\Sigma_z(\varphi(z)-\varphi^b)}. \tag{9}$$

As can be seen in Fig. 6, where we present our results for the depletion thickness as a function of the bulk volume fraction

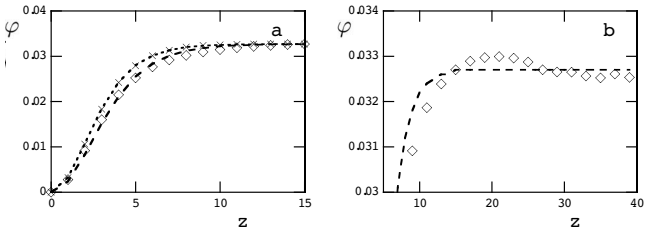

FIG. 5. Polymer concentration profiles obtained by the classical SCF (crosses), and the hybrid MC-SCF (diamonds) methods. Bulk concentration $\varphi^b=0.0327$, $N=1001$. The lines are the best fit of the form $\varphi(z)=\varphi^b\tanh^2(z/\xi)$ with $\xi=3.08$ (dot) and $\xi=3.61$ (dash). In panel a the profiles near the surface (small z values) are shown, whereas in panel b it is shown how the profile goes to the bulk value for the MC-SCF profile.

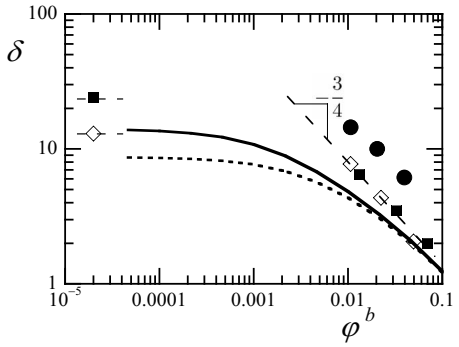

FIG. 6. Logarithm of depletion layer thickness vs logarithm of bulk polymer concentration. MC-SCF results for chain lengths $N=1001$ (squares), $N=401$ (diamonds). Dashed lines are added to guide the eye. Classical SCF results for chain lengths $N=1001$ (solid line), $N=401$ (dashed line), and results from Ref. 17 rescaled for $N=1000$ (circles). The theoretical slope $-3/4$ is indicated.

in log-log coordinates, we basically recover the expected behavior. At low polymer concentrations the results depend strongly on the chain length and the depletion layer is given by the radius of gyration of the chains: $\delta \approx R_g$. Above the overlap concentration the depletion thickness is no longer a function of the molecular weight but becomes a function of the polymer concentration only. Completely in line with expectations, in semidilute solutions a power-law dependence is found. A fit of the depletion layer thickness as a function of the polymer volume fraction in the bulk gives $\delta^{\text{MC-SCF}} \propto (\varphi^b)^{\alpha}$. Inspection of Fig. 6 proves that the MC-SCF results are consistent with $\alpha=-3/4$. As the depletion layer thickness is an accurate measure for the bulk correlation length, we note that $\alpha=-3/4$ is consistent with the scaling prediction of de Gennes.[3] This proves that the excluded volume interactions are reasonably accurately accounted for in the MC-SCF calculations.

This should be contrasted to the classical results of the mean field theory for which the value of $-1/2$ is found if the chains are long enough. For comparison with the classical SCF result we also present the classical result for the depletion thickness as a function of the polymer concentration in Fig. 6. Indeed relatively large differences between the classical SCF and the new MC-SCF results are observed, especially for low polymer concentrations. With increasing concentration, however, the differences diminish. Indeed, when the depletion thickness becomes of order of the segment size, that is in the concentrated regime, the MC-SCF results converge to the classical mean field results. This is expected because in the melt the mean field theory is known to be accurate. More specifically, the two results are expected to merge because both approaches are based on the same freely jointed chain model.

At this stage it is necessary to compare the MC-SCF results to computer simulations. To begin with, there are very limited accurate results available in the literature. The reason for this is clear. Basically, in order to arrive in the regime where the de Gennes scaling is expected one has to have long chains in the system. Moreover, one needs many chains in such a system and thus the necessary simulations are huge. In Fig. 6 we compare results to computer simulations by Bolhuis and co-workers.[17,18] It must be noted that these authors did not present atomistic simulation results but rather turned to a coarse graining strategy. These authors extend an earlier idea of Murat and Kremer[19] to replace a polymer chain by a single soft particle. They accurately measured the pair potentials between polymers and evaluated the depletion problem using these particles. As can be seen in Fig. 6 there are remarkable differences in absolute values between predictions by Bolhuis *et al.*,[18] and our results. Most likely these differences may be attributed to differences in chain models used. More specifically, in the Bolhuis simulations, while measuring their pair potentials the chains were fully self-avoiding, whereas in our SCF analysis the freely jointed chain model was used. The scaling of the depletion thickness with polymer concentration found by Bolhuis *et al.*[18] is the same as in our calculations and both are in agreement with the de Gennes scaling prediction.

We now shortly elaborate on the characteristics of the depletion profile as one would extract from the coarse grained MC simulations, that is, in the absence of the fine-graining step. In the MC simulations the polymer chain is essentially replaced by a single particle. The particle interact with the solid wall other particles via effective potentials calculated in the dilute regime. In semidilute regime these potentials are only approximately correct as they do not account for screening effects. Moreover, by using an isotropic radial volume fraction profile of such particle to calculate overall polymer concentration profile one strongly overestimates the width of the depletion layer and underestimates the depth of it. This is no surprise as to obtain accurate information on the depletion zone requires information on length scales smaller than the particle size. The error exemplifies the necessity for our fine-graining procedure.

The density profile for the depletion problem is not monotonically increasing, but a depletion layer is followed by a small overshoot followed by an even smaller undershoot, etc. [cf. Figure 5(b)]. Even though the overshoot is small it is well above the statistical noise. In principle these oscillatory features have been reported before and also exist to a lesser extend in the classical SCF results,[20] that is, in calculations that go beyond the GSA. These nonmonotonic profiles were also reported by Bolhuis *et al.*[17] Oscillatory density profile are perhaps best known for densely packed hard spheres near a flat interface. The softer the particles are the more the oscillations are damped. Polymer chains are very soft particles as may also be deduced from $F^w(h)$ and $F^{12}(d)$. Full overlap of coils however costs significant amount of entropy. Hence the particles have a finite softness and therefore there are small overshoots and undershoots visible in the profile. From a polymer point of view one can argue that the overshoot is the result of chain ends. Polymer ends can be inserted into the depletion zone more efficiently than middle segments, and therefore there is some "adsorption" affinity of the polymer chain to accumulate at the boundary of the depletion zone. We note that in dilute solution, when all chains interact with the surface individually, there is no possibility to develop an overshoot in the profile and also in the limit of an incompressible melt the overshoot

must vanish. Hence the amplitude of the overshoot is, in line with the results, a nonmonotonic function of the polymer concentration, and the chain length.

From the above we conclude that the MC-SCF method gives an improved description of inhomogeneous polymer solution over the classical SCF method. This improvement comes with a price. The computation time for the MC-SCF is estimated to be about J hours central processing unit (CPU) on a desktop personal computer per problem, as the CPU time per snapshot is approximately 1 h. Still the method is extremely efficient as the CPU time is linearly proportional to the volume of the system and the length of the polymer chains. The method is independent of the number of molecules n, if we ignore the fact that the value of J needed to average out fluctuations will be a weak function of n. In full scale simulations, on the other hand, the calculation time heavily depends on the length of the chains and further depends super linearly on the number of polymer chains in the solution. Also the number of snapshots needed to obtain an accurate estimate of some observable is much larger than in the MC-SCF method. Hence we claim that the CPU time gain of the present MC-SCF compared to MC may easily be significantly more than a factor 10^2 and this number grows quickly with system size.

One realistic target for future modeling is to study the adsorption of homopolymers and polyelectrolytes adsorbing from (semi)dilute solutions onto (charged) interfaces. The classical SCF method fails badly for many regimes, basically because it assumes that the chains in the bulk remain Gaussian (intramolecular excluded volume is basically ignored). In the limit of strong adsorption, however, we foresee that it may be more beneficial to use a hybrid Brownian dynamics (BD) SCF approach. In this approach we need for each time step the forces that act on the centers of mass of the particles. These forces can be found by solving the SCF equations, while keeping these central positions as constraints similarly as done in the MC-SCF method used above. The (time) averaging of results along a BD trajectory will allow us to outperform mean field theories, while keeping CPU time within bounds of modern computers.

At this stage it is worthwhile to pay attention to still relatively weak points of the MC-SCF method. To our mind the ansatz that just one positional constraint is used per chain is still a significant simplification of the real excluded volume problem. The next step to improve the situation is to specify two constraints per macromolecule, e.g., by assigning constraining positions to both end points of the chain. Without going into all computational details, it is evident that an implementation of this idea requires a measurement (in SCF mode) of the end-to-end "potential," $F^{e-e}(R)$ where R is the distance between the two ends of a probe chain. The MC step will be somewhat more complicated because there will be two times more degrees of freedom and one extra potential and the SCF part must be modified in order to prevent the exchange of end points between molecules. It is expected that the computation time per snapshot will not grow much for systems that feature molecules with two constraints but we can foresee a significant increase in number of snapshots needed to measure averaged properties of the system accurately. This idea can be extended. One may arrive at a model were one considers a string of blobs and then the method has several aspects in common with a recently suggested theoretically informed MC simulations by Detcheverry and co-workers.[21,22] In short these authors combine a particle-based MC method with interactions derived from a local density functional theory. Instead of solving the Edwards equation as in our case these authors implemented a still primitive smearing of the density to allow an easy evaluation of the interactions. Possibly, merging our MC-SCF method with theoretically informed simulations may be a feasible route to improve both methods.

Compared to classical MC simulation, the MC-SCF method has the intrinsic advantage that thermodynamic quantities can be calculated rather accurately. The idea is that for semidilute solutions of long enough chains the translational entropy is not important and one can simply average the free energy of the snapshots, i.e., $F^{\mathrm{SCF}}=\Sigma_j F_j^{\mathrm{SCF}}/J$. However, when for some system the translational entropy is important, one may get a reasonable estimate form the MC simulation using standard techniques.

IV. CONCLUSIONS

We have presented a hybrid MC-SCF approach for polymers in good solvent near a nonadsorbing surface. This method accounts for inter as well as intramolecular excluded volume effects and the results are consistent with scaling predictions. Compared to full scale simulations the method has modest computation times albeit that the computation costs are several orders of magnitude larger than the classical SCF method. The method introduces a MC step wherein a coarse grained simulation is performed, and a SCF step to recover the structural details on a shorter length scale (fine graining). In other words, conformational degrees of freedom are accounted for by the classical propagator method (analogous to the Edwards diffusion equation) for which the centers of mass are fixed to coordinates specified by the MC snapshot. The MC-SCF approach can be extended to further improve on the excluded volume problem in inhomogeneous systems. Alternative hybrid approaches are foreseen which may be used in the cases where the polymers are strongly perturbed with respect to the Gaussian size.

ACKNOWLEDGMENTS

Financial support from the EU POLYAMPHI/Marie Curie program (Grant No. RT6-2002, Proposal 505027) and European Science Foundation EUROCORES program collaborative BIOSONS is also acknowledged.

[1] A. A. Louis, P. G. Bolhuis, J. P. Hansen, and E. J. Meijer, Phys. Rev. Lett. **85**, 2522 (2000).
[2] G. J. Fleer, M. A. Cohen Stuart, J. M. H. M. Scheutjens, T. Cosgrove, and B. Vincent, *Polymers at Interfaces* (Chapman and Hall, London, 1993).
[3] P. G. De Gennes, *Scaling Concepts in Polymer Physics* (Cornell University Press, Ithaca, 1979).
[4] G. J. Fleer, A. M. Skvortsov, and R. Tuinier, Macromol. Theory Simul. **16**, 531 (2007).
[5] S. F. Edwards, Proc. Phys. Soc. Jpn. **85**, 613 (1965).
[6] G. H. Fredrickson and F. Drolet, Macromolecules **35**, 16 (2002).

[7] M. Muller and G. D. Smith, J. Polym. Sci., Part B: Polym. Phys. **43**, 934 (2005).
[8] G. J. A. Sevink, J. G. E. M. Fraaije, and H. P. Huinink, Macromolecules **35**, 1848 (2002).
[9] R. Elliott, K. Katsov, and M. Schick, J. Chem. Phys. **122**, 044904 (2005).
[10] J. M. H. M. Scheutjens and G. J. Fleer, J. Phys. Chem. **83**, 1619 (1979).
[11] J. van Male, "Self-consistent-field theory for chain molecules: extensions, computational aspects, and applications," Ph.D. thesis, Wageningen University, 2003.
[12] In the case of an even number of segments in the chain, we would have to assign one of the two central segments as the pinned segment. In this case the two chain fragments that are connected to the central segment differ in length by one segment.
[13] C. von Ferber, Yu. Holovatch, A. Jusufi, C. N. Likos, H. Löwen, and M. Watzlawek, J. Mol. Liq. **93**, 151 (2001).
[14] N. Metropolis, A. W. Rosenbluth, M. N. Rosenbluth, A. H. Teller, and E. Teller, J. Chem. Phys. **21**, 1087 (1953).
[15] Using individual profiles $\varphi_j(\mathbf{r})$, we computed for each coordinate $\mathbf{r}$ the standard deviation σ from the average $\bar{\varphi}(\mathbf{r})$. The numerical error reduces with the square root of the number of snapshots J.
[16] G. J. Fleer and F. A. M. Leermakers, in *Coagulation and Flocculation*, 2nd ed., edited by H. Stechemesser and B. Dobias (Surfactant Science Series, Boca Raton, FL, 2005), p. 349.
[17] P. G. Bolhuis, A. A. Louis, J. P. Hansen, and E. J. Meijer, J. Chem. Phys. **114**, 4296 (2001).
[18] P. G. Bolhuis *et al.* have presented their results in reduced units. They normalized the depletion thickness by the radius of gyration and the concentration by the overlap concentration. We used Eq. 9 in Ref. 17 to transform their results to the units used in Fig. 6.
[19] M. Murat and K. Kremer, J. Chem. Phys. **108**, 4340 (1998).
[20] J. van der Gucht, N. A. M. Besseling, J. van Male, and M. A. Cohen Stuart, J. Chem. Phys. **113**, 2886 (2000).
[21] F. A. Detcheverry, D. Q. Pike, P. F. Nealey, M. Mueller, and J. J. de Pablo, Phys. Rev. Lett. **102**, 197801 (2009).
[22] D. Q. Pike, F. A. Detcheverry, M. Mueller, and J. J. de Pablo, J. Chem. Phys. **131**, 084903 (2009).